



Finite Element Analysis on The Effect of Gap Between Masonry Infill and Reinforced Concrete Frame Under Inplane Loading

Author 1:

Name: Md. Munirul Islam

Affiliation: Assistant Professor, Department of Civil Engineering, Ahsanullah University of Science and Technology, Bangladesh.

Email: saeedce@yahoo.com

ORCID No: 0000-0003-3449-6609

Author 2:

Name: Debasish Sen

Affiliation: Assistant Professor, Department of Civil Engineering, Ahsanullah University of Science and Technology, Bangladesh.

Email: dsendip@gmail.com

ORCID No: 0000-0001-6375-4596

Author 3*:

Name: Sharmin Reza Chowdhury

Affiliation: Professor, Department of Civil Engineering, Ahsanullah University of Science and Technology, Bangladesh.

Email: chowdhury.ce@aust.edu

ORCID No: 0000-0001-5227-3463

*Corresponding author: chowdhury.ce@aust.edu

Received: 27/04/2024
Revised: 16/09/2024
Accepted: 02/10/2024

ABSTRACT

The lateral force-resisting system of many buildings in Bangladesh and worldwide comprises masonry-infilled reinforced concrete frames. Previous studies have demonstrated that an inadvertent (for poor workmanship) or intended gap between the frame and infill can significantly alter the inplane strength and stiffness of the infilled frame system. Only a few studies used reinforced concrete frames. The criteria for the size and position of the gaps were likewise constrained. The main goal of this study is to numerically investigate the impact of the gap between the reinforced concrete frame and the masonry infill at various locations and in various magnitudes (i.e., column gap (s), beam gap, and all sides gap). Using ABAQUS, a finite element model of a reinforced concrete frame with masonry infill was produced utilizing the macro technique to simulate the masonry panel in order to examine the impact of gaps on the inplane behaviour and strength of masonry infills bound by frames. The investigation of the global behaviour was carried out in terms of lateral load and story drift response, initial stiffness reduction ratio, and ultimate strength reduction ratio. Investigation results showed that lateral stiffness and strength decreased by 28-70% and 5-11% respectively, when aforementioned gaps were considered. The reduction trend was validated with experimental results.

KEYWORDS

RC frame, infilled masonry, gap, stiffness reduction, and strength reduction.

1. Introduction

Masonry is among the oldest materials used in building construction. Masonry buildings have existed since the beginning of humanity. Typically, masonry partitions are regarded as non-structural components. For moderate amounts of inplane lateral load, masonry walls inside a RC frame may cooperate with the frame to give maximum rigidity (Islam, 2022). Since it satisfies all architectural requirements, including effective thermal and acoustic insulation, durability, and simple and affordable construction, the use of masonry wall as interior and exterior partitions is frequently the preferred alternative (Ferraioli, 2020). In several nations, including Bangladesh, these RC frames with masonry infill are frequently used (Islam and Chowdhury, 2020). Masonry partitions are typically considered non-structural elements. Nonetheless, previous studies (Sen et al., 2024; Islam et al., 2022; Khuda, 2022; Faisal et al., 2022) have shown that masonry infills can improve the lateral stiffness and load-bearing capacity of reinforced concrete (RC) frames, though they may also compromise the frames' ductility. Recent destructive earthquakes have highlighted the notable contribution of masonry infills on the seismic performance of reinforced concrete (RC) buildings (the L'Aquila earthquake in 2009, the Emilia earthquake in 2012, the Peru earthquake in 2007, the Sichuan earthquake in 2008, and the İzmit earthquake in 1999). Masonry panels interact with the nearby RC components during an earthquake, and the combination of their high stiffness

and brittleness may severely impact the structure's seismic performance. The infill wall may cause additional lateral strains to some structural components, such as columns, which is another unfavorable effect of the infill wall (Barnaure and Stoica, 2015). A gap between the reinforced concrete frame and the masonry infill is also regarded as crucial because the masonry infill panels occasionally serve as a structural component. It is not unusual for there to be a gap between the reinforced concrete frame and the masonry infill. In the real world, these gaps are non-uniform and unintentional. The shrinkage and settlement of the infill or flaws in the workmanship are typically responsible for the gaps. Sometimes intentional gaps are provided to prevent column damage during earthquakes. Since the intentional gap considerably impacts the reinforced concrete frame's overall behaviour, it is essential to consider its effect. When there is no interaction between the frame and the infill, the structure responds in the same way as a bare frame; but, once there is contact, there is a sharp increase in stiffness, and the structure behaves more like the fully infilled one (Barnaure and Stoica, 2015). Previous research on masonry infilled frames (Nazief, 2014; Hu, 2015; Steeves, 2017; Sonpal, 2018; Chen, 2015) has demonstrated that an inadvertent (because of poor workmanship) or intentional gap between the infill and the RC frame can significantly affect the inplane strength and stiffness of the infilled frame system. Nazief (2014) executed finite element modelling where the gap has been introduced within a range from 5 mm to 15 mm at the top and on all sides between the reinforced concrete (RC) frame and the masonry infill. The study observed hardly any reduction in initial stiffness for gaps at the top, whereas gaps on all sides led to a significant reduction of 55% to 90%. The ultimate strength was found to decrease by 12% to 20% for specimens with top gaps and by 30% to 64% for specimens with all side gaps. Hu (2015) conducted a test using a concrete masonry unit, incorporating 7 mm and 12 mm gaps at the top and side between the RC frame and the masonry infill. The obtained results indicated a reduction in initial stiffness of 28% for specimens with top gaps and 31% for those with side gaps. Additionally, the ultimate strength decreased by 22% for the top-gapped specimens and 14% for the side-gapped specimens. Meanwhile, Steeves (2017) introduced a 25 mm gap at the top and a 12 mm full gap between the RC frame and the masonry infill and compared the obtained results with the control model of Hu (2015). The ultimate strength for all side-gapped specimen was 28% lower and a 25 mm top gap specimen exhibited a reduction of about 30% when compared to the strength of a frame without gaps. Sonpal (2018) carried out finite element modelling on ANSYS where he introduced 5 mm, 10 mm, and 15 mm gaps at the sides between the RC frame and masonry unit. In the analysis, the initial stiffness was reduced by 23% on average, and the ultimate strength was reduced by 63% on average. Chen and Liu (2017) also conducted an analytical study on infilled steel frames using the ANSYS software. The obtained findings indicated that gaps between beams and infill had a more significant effect on lateral load capacity compared to gaps between columns and infill. Additionally, the influence of interfacial gaps was less pronounced in weaker frames compared to stronger ones.

The literature survey demonstrates that few researchers took comprehensive endeavours to experimentally investigate the effect of the gap between masonry and RC frame on the lateral behaviour of masonry-infilled RC frame. Additionally, previous studies concentrated on gaps on one or two specific sides only. A comprehensive analysis covering gaps at all possible locations between the reinforced concrete (RC) frame and the infill was not included. Since the experimental endeavour is expensive and time-consuming, a comprehensive numerical investigation has been

designed to investigate the effect of the gap in the masonry-infilled RC frame. The overall behavior of the masonry-infilled frame is evaluated without and with gaps. This study will help practicing engineers to perceive the effect of the gap between infill wall and frame on the lateral behavior of masonry-infilled RC frame. In addition, it will provide a tentative idea of how much of a gap is permissible. This kind of comprehensive study on the effect of the gap is lacking in existing literature, therefore this study will contribute in this regard. This study primarily aims:

1. To carry out a parametric analysis of the impact of infilled RC frames under various mortar grades of masonry panel.
2. To investigate the effect of the gap between the masonry wall and the surrounding RC frame at different locations with different magnitudes focused on the infilled frame's lateral stiffness and lateral strength.

2. Finite element modelling

The finite element modelling of RC frame and masonry infill is done using the finite element software ABAQUS 6.14. Using reference test specimens found in the available literature (Seki et al. 2018), the bare frame and masonry-infilled RC frame models are created, and their lateral behaviour is validated using the results of experimental tests (Islam et al., 2023).

According to Seki et al. (2018), a half-scale RC bare frame measuring 2250 x 1950 mm was analyzed, consisting of two rectangular columns (25x25 cm) with 4 ϕ 12 mm longitudinal reinforcements and ϕ 8 mm tie reinforcements of 30 cm spacing. A second specimen featured the same RC frame configuration but included a masonry infill panel, as illustrated in **Figure 1**. The masonry infill was constructed using burned clay bricks with a thickness of 115 mm.

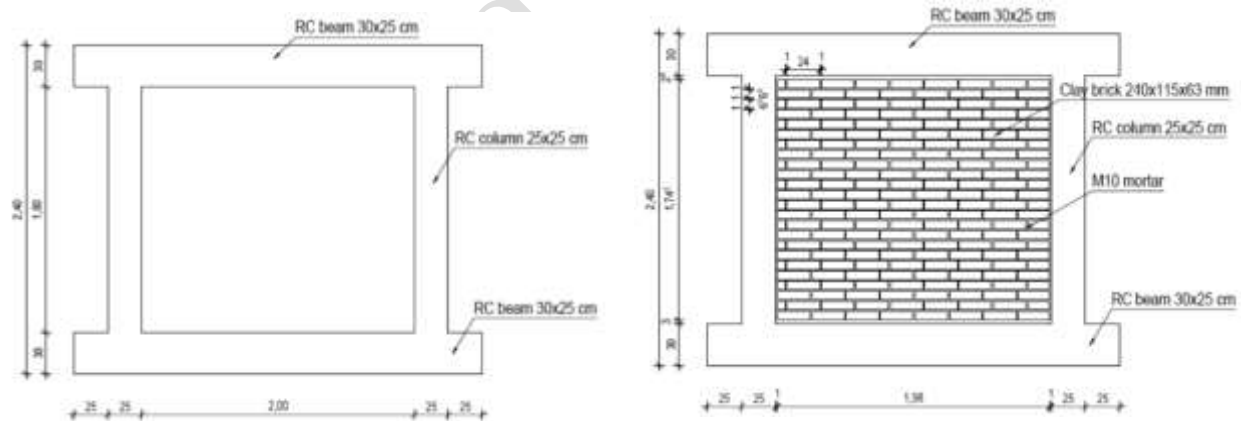


Fig. 1. The reinforced concrete bare frame and Masonry infilled RC frame (Seki et al., 2018) [All dimensions are in cm]

Initially, an RC bare frame and masonry-infilled RC frame are developed in ABAQUS and verified with the reference test specimen by Seki et al. The details of finite element modelling and verification are discussed in the study of Islam et al. (2023). After verifying the models with the experimental reference data, the same MIF model was further analyzed with different gap sizes at various locations between the RC frame and masonry panel to investigate the effect of the gap.

RC frame

In the current study, Concrete Damaged Plasticity (CDP) is utilized as a constitutive model for concrete. Concrete was modeled using eight-node, three-dimensional hexahedral brick elements (C3D8R), which feature reduced integration and three translational degrees of freedom per node. This element is able to model the nonlinear behavior of concrete. Several researchers already used this element to model concrete (Ali et al., 2023; Schäfer et al., 2020; Islam, 2022; Abbas and Awazli, 2017). Carriera and Chu's uniaxial compression model (Carriera and Chu, 1985) is used to generate the concrete's effective stress-strain curve as shown in **Figure 2**. Poisson's ratio of concrete is considered as 0.18. The biaxial-to-uniaxial compressive yield stress ratio, eccentricity, and viscosity were among the parameters for the concrete damage plasticity model that were taken from the default values given in the ABAQUS documentation. The dilation angle of concrete has been considered as 31° in this FE model. Truss elements T3D2, which are embedded in concrete throughout the frame, were used to represent the longitudinal and transverse reinforcement. These elements consist of two nodes. Both reinforcements are modeled considering a bilinear model of steel where the cracking strain property was set to 0.17, while Poisson's ratio was assumed to be 0.3, based on values provided in the ABAQUS documentation. More details of the adopted material properties of the finite element models are discussed in the authors' prior study (Islam et al., 2023).

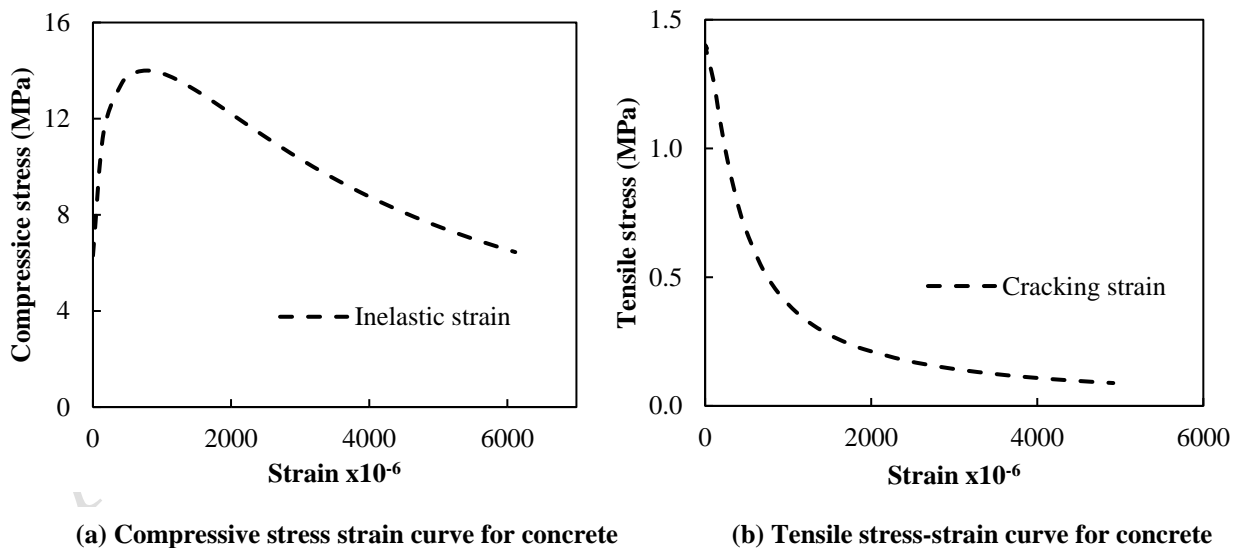


Fig. 2. Stress vs Strain curve for concrete (Islam, 2022)

The longitudinal and tie reinforcements are referred to be "embedded" in the concrete as constraints to help bind the concrete to the reinforcing bars. This makes it possible to connect the rebar's activity with the nearby concrete mass. The purpose of tie constraint at the beam-column

junction is to create a link between the top of the column and the bottom surface of the beam. In **Figure 3 (a)**, the constraints are illustrated. Similar to the experimental loading methodology of Seki et al. (2018), all specimens were subjected to a continuous axial load of 350 kN on each column and a 50 mm of monotonic lateral displacement (2.5% height) from the left side (push). The 350 kN axial load is applied in the FE model as a normal stress of 5.6 N/mm^2 on an upper surface top beam (i.e., the projected area of the column's cross-section) as shown in **Figure 3(b)**. The boundary conditions of the model are specified in the restraints section. As shown in **Figure 3(b)**, every node at the base of the columns is completely restrained in every direction, preventing both rotation and translation.

According to the test results of the RC frame, the lateral resistance measured is 81 kN, at 1% story drift. The maximum lateral resistance for the bare frame in the finite element model, 79.37 kN, is reached at 0.7% lateral drift. The initial stiffness of the bare frame (at 0.1% drift) was 12.82 kN/mm for the experimental model and 15.38 kN/mm for the finite element model. The validation graph of the bare frame is shown in **Figure 4**.

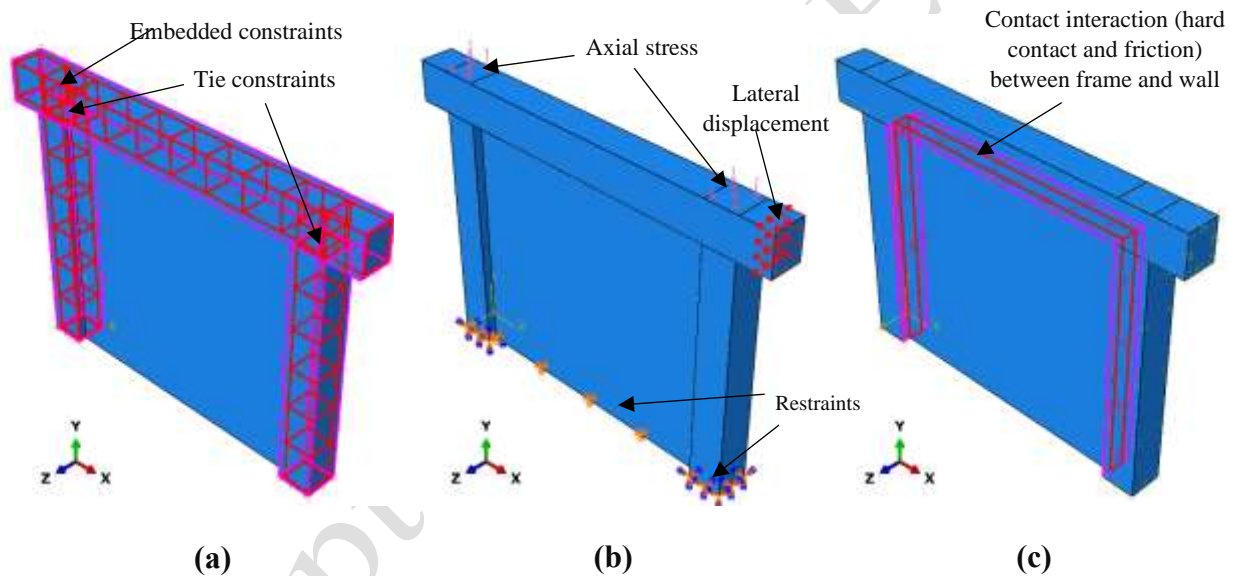


Fig.3. All types of (a) Constraints, (b) Restraints, and (c) Interaction considered in FE models (Islam, 2022)

Masonry infilled frame

The RC frame was modelled in a similar manner and the masonry wall was modelled utilizing the macro model. A plasticity model of the Drucker-Prager type is used to simulate the behaviour of masonry (Drucker and Prager, 1952). **Table 1** presents the material parameters of masonry. As the RC frame surrounds the masonry panel, both the RC frame and the masonry will interact when the lateral load is applied. In order to accomplish this, a "contact" interaction with a friction coefficient of 0.7 is assigned between the inner surface of the RC frame and the outer surface of the masonry panel. In addition, hard contact is considered at the interface of the RC frame and masonry infill. The interaction between the frame and the masonry wall is shown in **Figure 3 (c)**.

Table 1.Material properties of masonry(Islam et al., 2023)

Material properties	Values
Compressive strength (MPa)	11.6
Modulus of Elasticity (MPa)	6380
Poisson's Ratio	0.2
Angle of friction	31.79
Flow stress ratio	0.8
Dilation Angle	2.86
Shear strength (MPa)	0.58

The frame with masonry infill had a maximum lateral load of 156 kN, at 1% lateral drift. The maximum lateral load for the masonry infilled frame from the finite element model is 147.62 kN at 1.1% story drift with a 5.37% difference which is fairly close to the experimental results. **Figure 4** shows the lateral strength and story drift relationship obtained experimentally and FEM analysis of the bare frame and masonry-infilled frame.

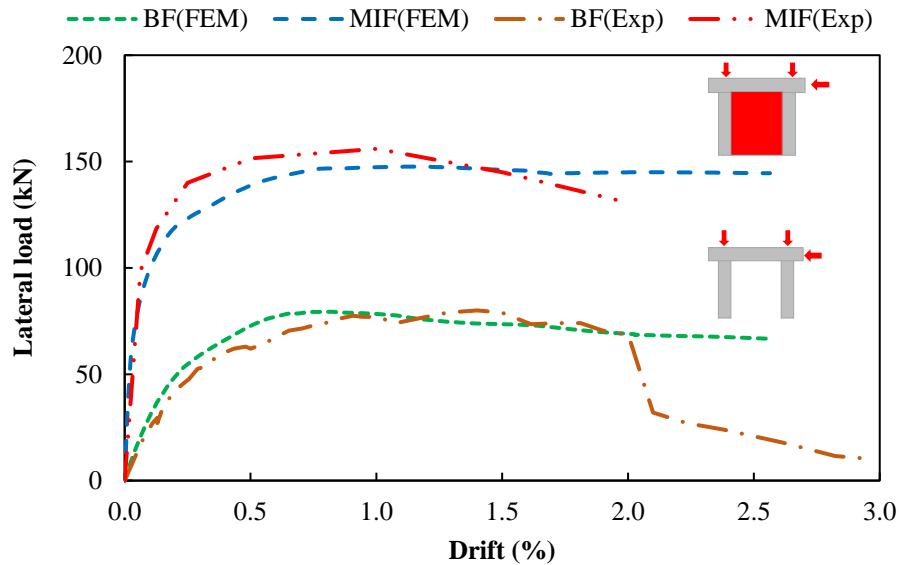


Fig.4.Relationship of lateral strength and story drift of bare frame and masonry-infilled RC frame (Islam et al., 2023)

3. Parametric study on masonry infilled frame

After validating the masonry-infilled RC frame, a parametric study on masonry masonry-infilled frame is done by varying the grades of mortar. According to BNBC 2020, there are six grades of mortar (M1 to M6). The inherent property of masonry that can be utilized in the design of various masonry elements is prism strength, f_m (Kahrizi et al., 2022). The prism strength of masonry, f_m

varies widely due to the combination of bricks and mortars. In the literature, various approaches to f_m calculation are described. Kaushik et al. (2007) carried out several experimental investigations to evaluate the uniaxial compressive stress-strain curves of brick units, mortar cubes, and masonry prisms with various combinations of brick and mortar grades. According to him, the prism strength of masonry can be calculated from **Equation 1**.

$$f_m = 0.63f_b^{0.49}f_j^{0.32} \quad [1]$$

where f_b is the compressive strength of brick and f_j is the compressive strength of mortar.

The compressive strength of 1st class brick is considered as 10.3 N/mm². The modulus of elasticity (E_m) of masonry is calculated from BNBC 2020 which is shown in **Equation 2** and according to Alwashali et al. (2016), the shear strength of masonry (τ) is calculated from **Equation 3**.

$$E_m = 750f_m \quad [2]$$

$$\tau = 0.05f_m \quad [3]$$

Table 2. Prism strength, modulus of elasticity, shear strength of masonry, and lateral strength of masonry infilled frame from a different grade of mortar (Islam, 2022).

Grade of Mortar	Compressive strength of mortar (N/mm ²)	Compressive strength of brick (N/mm ²)	Prism strength of masonry (N/mm ²)	E_m (N/mm ²)	τ (N/mm ²)	Lateral strength of masonry infilled frame (N/mm ²)
M1	10	10.3	4.127	3095.25	0.206	105.71
M2	7.5		3.764	2823.00	0.188	103.51
M3	5		3.306	2479.50	0.165	100.78
M4	3		2.807	2105.25	0.140	98.03
M5	2		2.466	1849.50	0.123	95.96
M6	1		1.975	1481.25	0.099	93.09

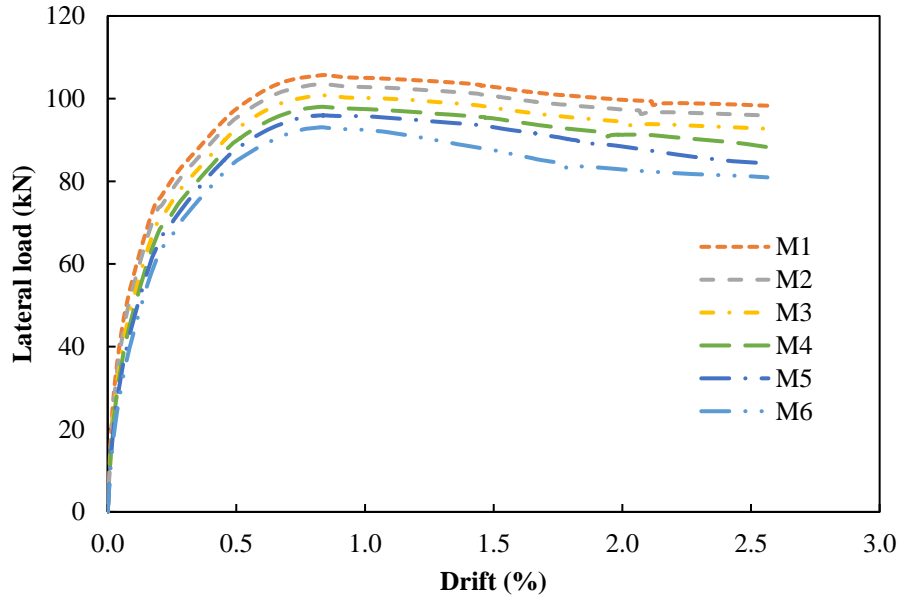


Fig.5.Effect of the grade of mortar according to BNBC 2020 (Islam, 2022)

Figure 5 shows that the higher the mortar grade, the higher the lateral strength of the frame since masonry prism strength increases with the mortar grade. The initial stiffness of all the graphs is almost the same, but their ultimate strength varied from 93.09 kN to 105.71 kN.

4. Effect of Gap Between Masonry Infill and RC Frame

This study categorizes the gap between masonry infill and RC frame into four groups. The details of all the numerical models have been presented in **Table 3** according to the varying parameters. In group 1 (RC5 to RC15), a gap is provided between the masonry panel and the right column. All the model parameters are kept constant, but the gap between the masonry panel and the right column varies from 5 mm to 15 mm. In group 2 (RC2.5-LC2.5 and RC5-LC5), a gap is provided between the masonry panel and both sides of the columns. Gaps at both sides of 2.5 mm to 5 mm are used as varying parameters. In group 3 (TB5 to TB15), a gap is provided between the masonry panel and the top beam. All the model parameters are kept constant, but the gap between the masonry panel and the top beam varies from 5 mm to 15 mm. In group 4 (AS2.5 and AS5), a gap between the masonry panel and the RC frame is provided at all sides. Gaps at all sides of 2.5 mm to 5 mm are used as varying parameters.

Table 3.Summary of frame model

Group	Model name	Masonry panel dimension		Gap location	Sample schematic model
		Length (mm)	Height (mm)		
-	BF (Islam, 2023)	-	-	N/A	
-	MIF (Islam, 2023)	2000	1800	N/A	
1	RC5	1995	1800	5 mm at right side	
	RC10	1990	1800	10 mm at right side	
	RC15	1985	1800	15 mm at right side	
2	RC2.5-LC2.5	1995	1800	2.5 mm at both sides	
	RC5-LC5	1990	1800	5 mm at both sides	
3	TB5	2000	1795	5 mm at top	
	TB10	2000	1790	10 mm at top	
	TB15	2000	1785	15 mm at top	
4	AS2.5	1990	1797.5	2.5 mm at all side	
	AS5	1990	1795	5 mm at all side	

BF = Bare frame, MIF = Masonry-infilled frame, RC = Right column, LC = Left column, TB = Top beam and AS = All sides

5. Results and discussion

The findings emphasize on how gaps of various sizes and locations affect the infilled frames' initial stiffness and final strength. The ratio of initial stiffness (0.1% drift) and the ratio of ultimate strength are calculated using the following **Equations 4** and **5**. And % initial stiffness and ultimate strength reduction are calculated using **Equations 6** and **7**.

$$\text{Stiffness reduction ratio, } K_r = \frac{K_{Gap}}{K_{MIF}} \quad [4]$$

$$\text{Strength reduction ratio, } Q_r = \frac{Q_{Gap}}{Q_{MIF}} \quad [5]$$

$$\% \text{ Reduction of initial stiffness} = \frac{K_{MIF} - K_{Gap}}{K_{MIF}} \times 100 \quad [6]$$

$$\% \text{ Reduction of ultimate strength} = \frac{Q_{MIF} - Q_{Gap}}{Q_{MIF}} \times 100 \quad [7]$$

where, K_{GAP} = initial stiffness from gap model, K_{MIF} = initial stiffness of masonry-infilled RC frame, Q_{GAP} = ultimate strength from gap model, Q_{MIF} = ultimate strength of masonry-infilled RC frame.

5.1 Gap at the right column

A gap between the masonry infill and the right column is shown in **Figure6**. The overall behaviour of the RC5, RC10, and RC15 models is shown in **Figure7**. For group 1 (RC5 to RC15) models, as there is no contact between the right column and the masonry panel, initially, it behaves like a bare frame (BF) with a slightly higher stiffness than the RC bare frame. The frictional resistance between the beam soffit and the top masonry course is probably what is responsible for this extra rigidity. The model started to exhibit an increase in stiffness as the infill started to contribute to the system stiffness as the load kept increasing and the lateral displacement increased to close the initial gap at the loaded side.

For the RC5 model, the initial stiffness is found 36.92 kN/mm, 28 % less than the initial stiffness of the masonry-infilled RC frame (MIF). After contact, its stiffness rises and reaches its ultimate strength, 5.09 % less than the ultimate strength of the masonry-infilled RC frame with no gap (MIF). A similar type of behaviour is observed for RC10 and RC15 models. The initial stiffness ratio and the ultimate stiffness ratio vs. the side gap is shown in **Figure8**. The initial stiffness ratio for RC5, RC10, and RC15 models are the same, and the ratios of ultimate strength for those models are hardly changed.

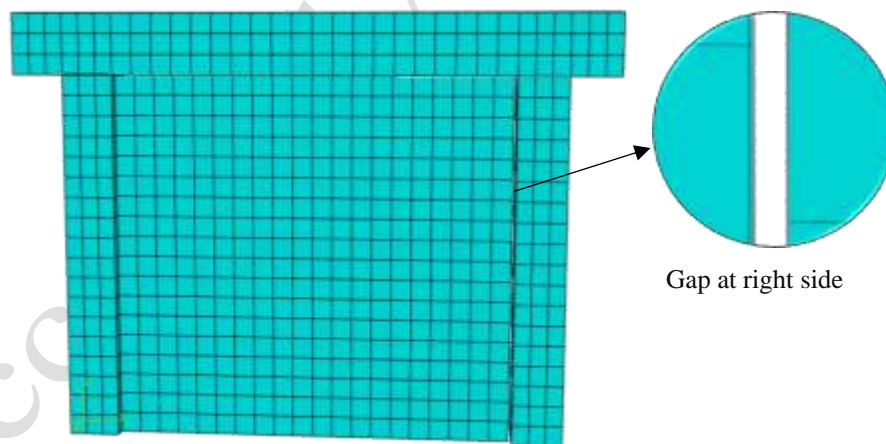


Fig.6. Gap between masonry infill and right column

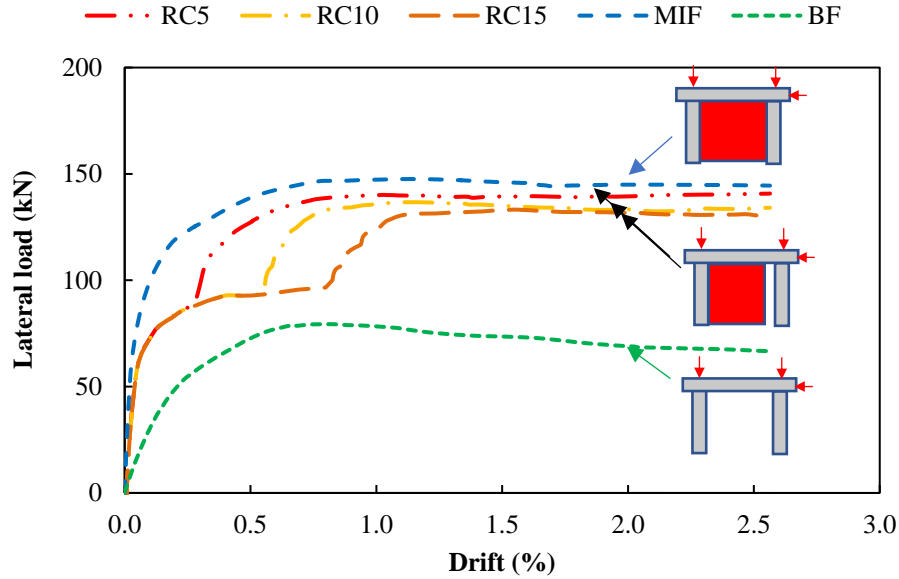


Fig.7.Effect of the gap at right side of the column

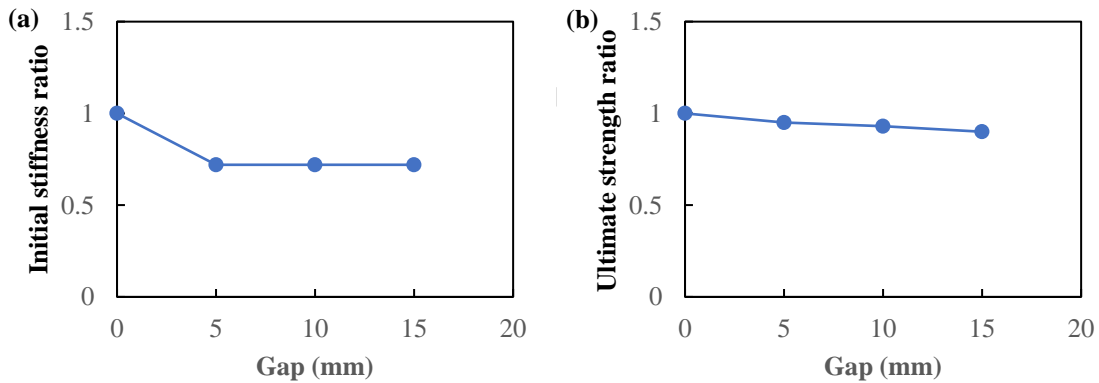


Fig.8.Relationship between the right-side gap size and (a) the initial stiffness ratio, (b) and the ultimate strength ratio

5.2 Gap at both sides of the column

Agap between the masonry infill and both sides of the column is shown in **Figure9**. The overall behaviour of RC2.5-LC2.5 and RC5-LC5 models is shown in **Figure10 (a)**. As there is no initial contact between the masonry panel and columns, these models performed similarly to a bare frame (BF) but with higher rigidity initially. Extra stiffness is anticipated by frictional resistance between the beam soffit and top masonry coarse. Although there is still a gap between the masonry infill and the right column, it closed due to increased lateral displacement and started to stiffen.

The initial stiffness for both RC2.5-LC2.5 and RC5-LC5 models is 36.92 kN/mm, 28 % less than the initial stiffness of the masonry-infilled RC frame (MIF). After contact, its stiffness rises and reaches the ultimate strength of 5.19 % less for the RC2.5-LC2.5 model and 8.12 % less for the RC5-LC5 model than the ultimate strength of the masonry-infilled RC frame (MIF). The

behaviour of RC5 is compared with RC2.5-LC2.5, shown in **Figure 10(b)**. Also, the behaviour of RC10 is compared with RC5-LC5, shown in **Figure 10(c)**.

The comparison found that, after contact, the rise of stiffness started at different drifts for both-sides gapped models (RC2.5-LC2.5 and RC5-LC5) and right-side gapped models (RC5 and RC10). Still, each model's initial stiffness and ultimate strength are found almost identical, as the total size of the gap is the same.

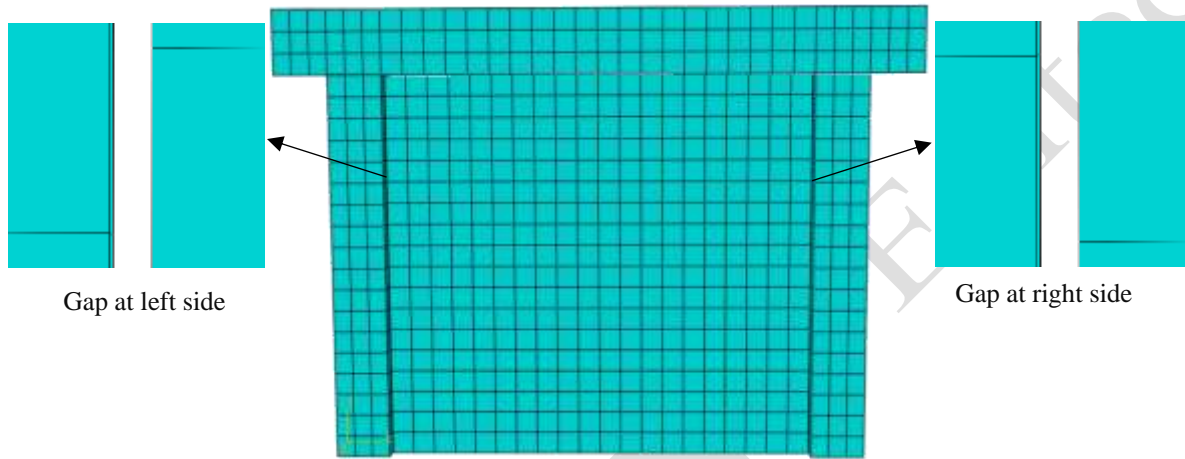
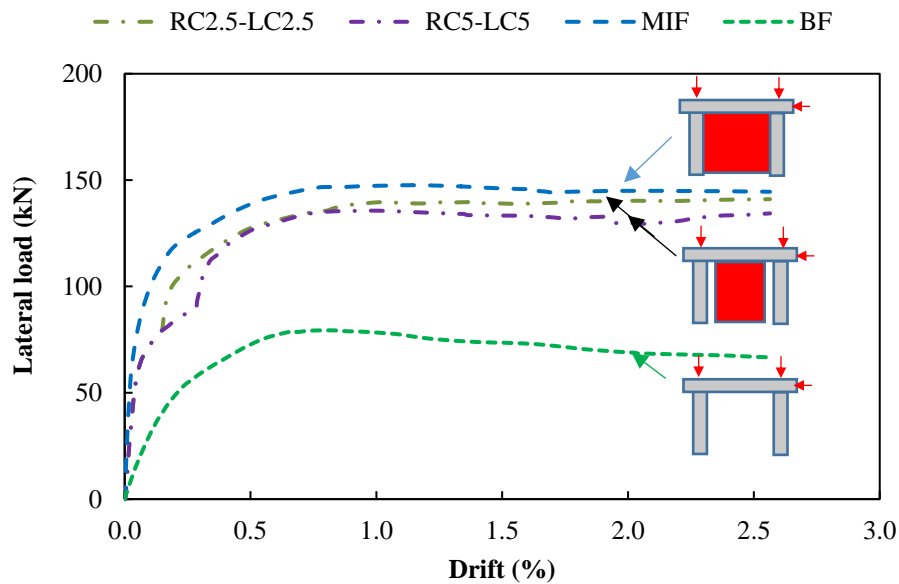
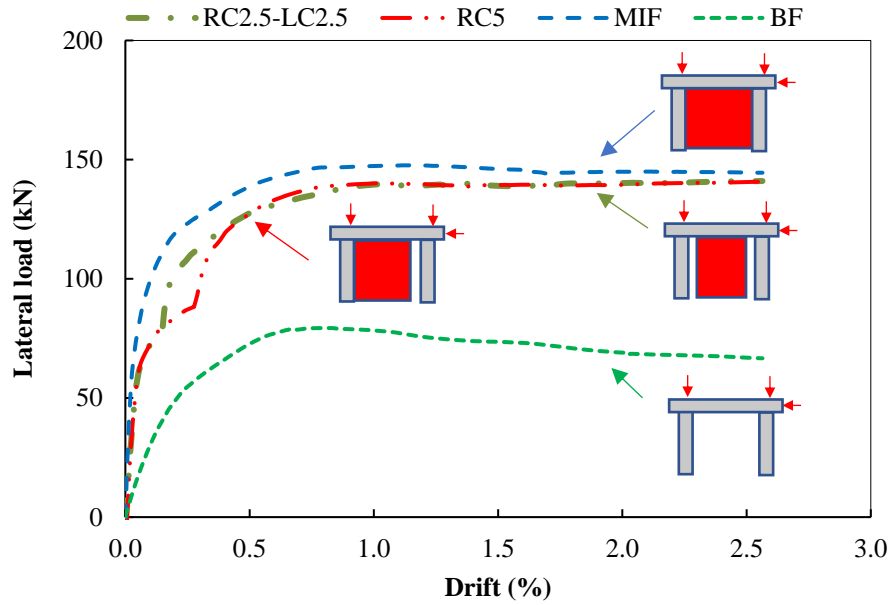


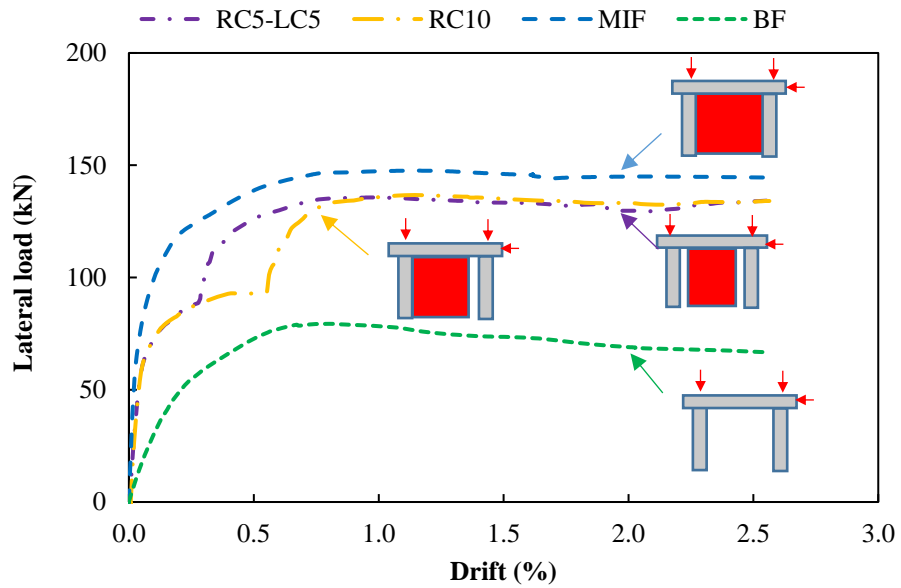
Fig.9. Gap between masonry infill and both sides of the column



(a) Relationship of lateral strength and story drift for model RC2.5-LC2.5 and RC5-LC5



(b) Relationship of lateral strength and story drift for model RC2.5-LC2.5 and RC5



(c) Relationship of lateral strength and story drift for model RC5-LC5 and RC10

Fig. 10. Effect of the gap at both sides of the column

5.3 Gap at the top beam

A gap between the masonry panel and the beam is shown in **Figure11**. The overall behaviour of TB5, TB10, and TB15 models is shown in **Figure12**. Initially, as it is already in contact with the columns, with the increase of lateral displacement, stiffness rises like a masonry-infilled frame (MIF), however the ultimate strength was hardly reduced at the final stage.

For the TB5 model, the initial stiffness is found 41.02 kN/mm. The reduction of initial stiffness was 20 % less than the initial stiffness of the masonry-infilled RC frame (MIF), but the ultimate strength reduction was only 5.26 %. Similar behaviour is observed for TB10 and TB15 models. The initial stiffness ratio and the ultimate stiffness ratio vs. the top gap is shown in **Figure13**. The initial stiffness ratio for TB5, TB10, and TB15 models are the same, and the ratios of ultimate strength for those models are hardly changed.

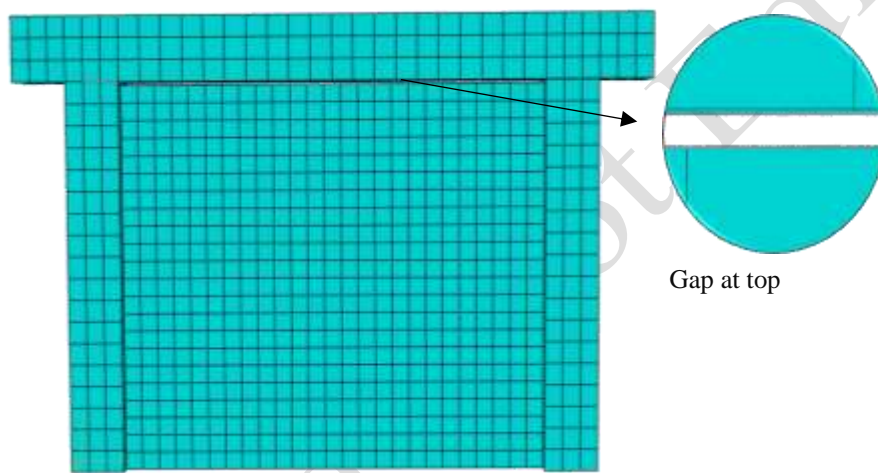


Fig.11.Gap between masonry infill and top beam

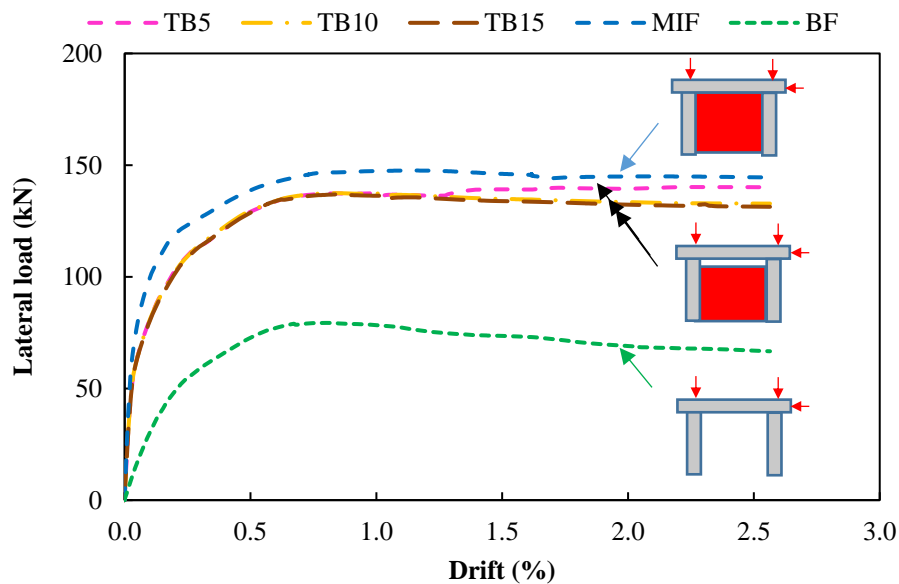


Fig.12.Effect of the gaps at the top beam

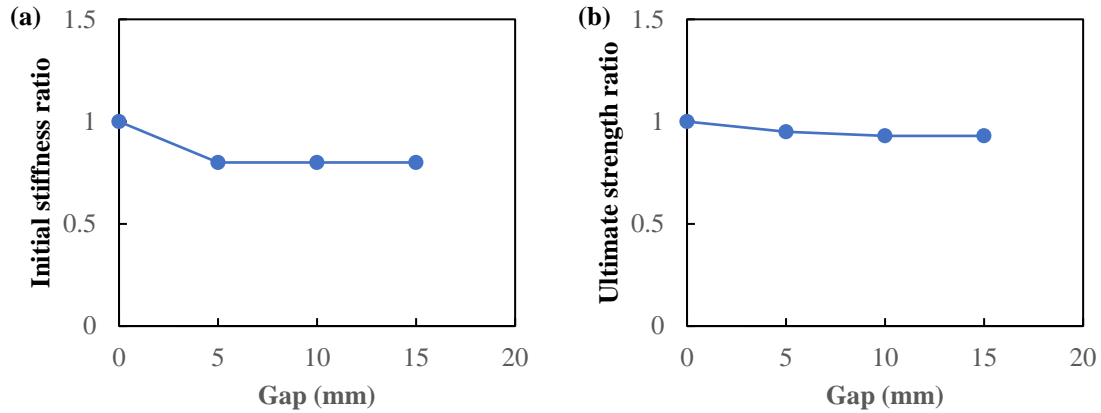


Fig.13.Relationship between the top gap size and (a) the initial stiffness ratio, (b) the ultimate strength ratio

5.4 Gap at all sides of the frame

For the AS2.5 model, a 2.5 mm gap and AS5 model, a 5 mm gap, are considered at all interfaces depicted in **Figure 14**. The overall behaviour of the AS2.5 and AS5 models is shown in **Figure 15 (a)**. As there is no contact between the masonry wall and the frame, initially, the model performed similarly to a bare frame (BF). The gap between the right column and the masonry infill closed and started to get stiffer as the lateral displacement increased.

The initial stiffness for both AS2.5 and AS5 models is 15.38 kN/mm, the same as the bare frame (BF) but 70 % less than the masonry-infilled RC frame (MIF). After contact, its stiffness rises and reaches the ultimate strength of 6.54 % less for AS2.5 and 10.96 % less for AS5 than the ultimate strength of the masonry-infilled RC frame (MIF). A comparison behaviour of models AS5, RC5-LC5, and TB5 is shown in **Figure 15(b)**.

The comparison found that the initial stiffness for mode TB5 and RC5-LC5 is 41.02 kN/mm and 36.92 kN/mm, respectively, which is close, but the initial stiffness for AS5 is 15.38 kN/mm, which is similar to the bare frame (BF). The rise of stiffness started for models RC5-LC5 and AS5 at a different stage. The ultimate strength reduction model TB5, RC5-LC5, AS5 models are 5.09 %, 8.12 %, and 10.96 %, respectively.

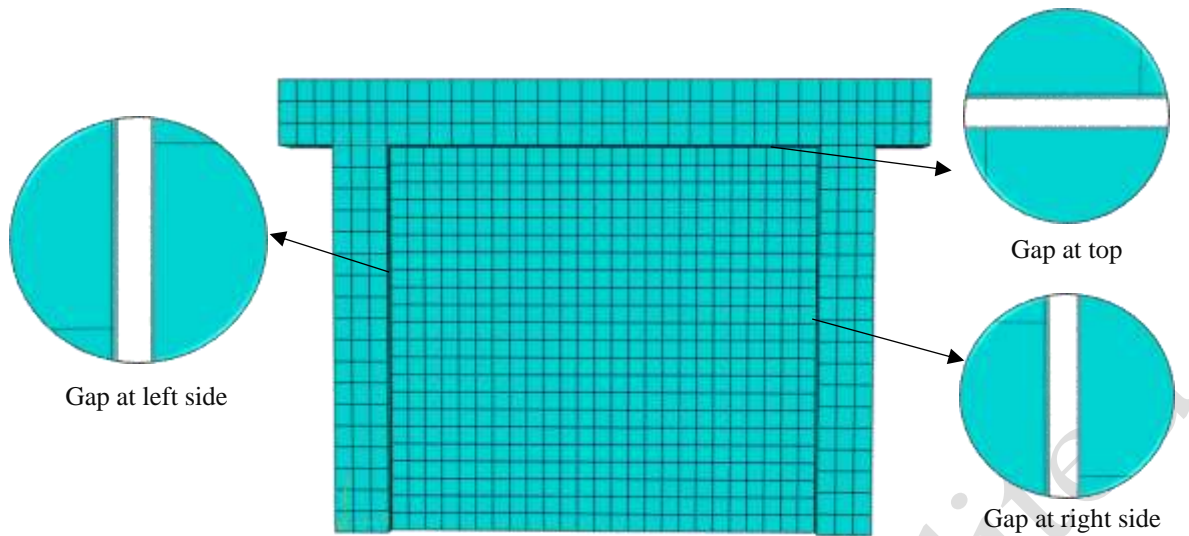
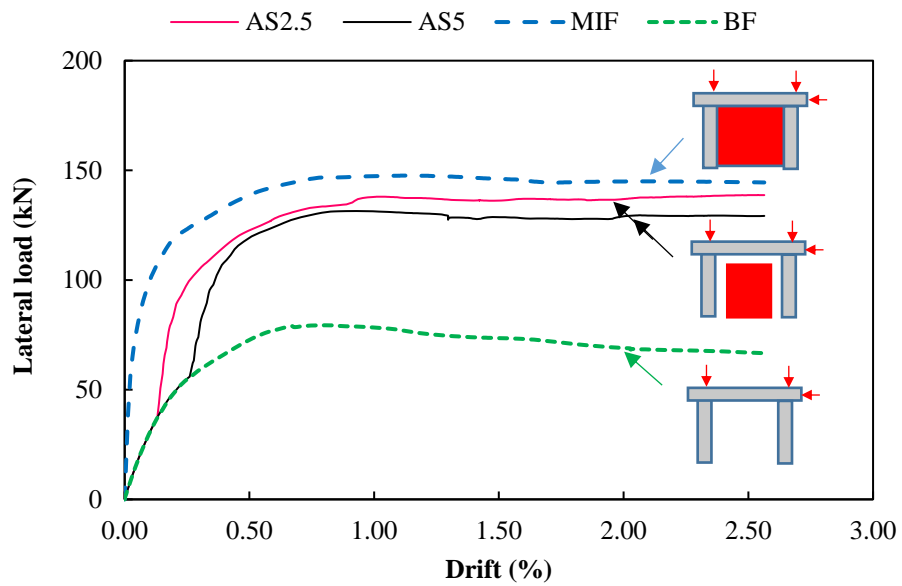
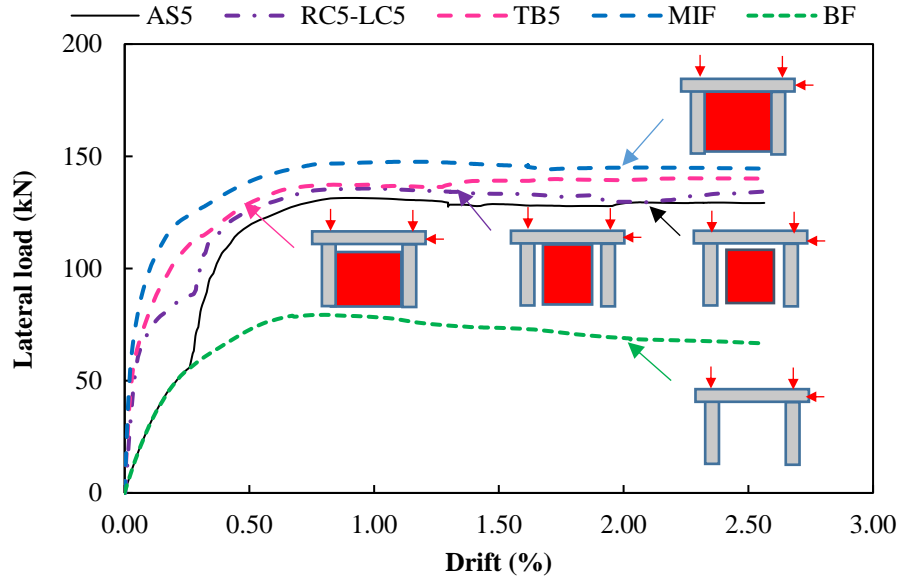


Fig.14.Gap at all sides between masonry infill and RC frame



(a) Relationship of lateral strength and story drift for model AS2.5, and AS5



(b) Relationship of lateral strength and story drift for model AS5, RC5-LC5, and TB5

Fig. 15. Effect of the gap at all sides

5.5 Discussion on the effect of all types of gaps:

The overall summary of the investigation of the gap between the masonry wall and RC frame at different locations with different magnitudes is presented in **Table 4**. The results are based on the initial stiffness and ultimate strength ratios.

Table 4. Effect of the gap on initial stiffness and ultimate strength

Model	Initial stiffness		Ultimate strength	
	Reduction %	Ratio (K_r)	Reduction %	Ratio (Q_r)
RC5	28	0.72	5.09	0.95
RC10	28	0.72	7.38	0.93
RC15	28	0.72	9.78	0.9
RC2.5-LC2.5	28	0.72	5.19	0.95
RC5-LC5	28	0.72	8.12	0.92
TB5	20	0.8	5.26	0.95
TB10	20	0.8	6.88	0.93
TB15	20	0.8	7.49	0.93
AS2.5	70	0.3	6.54	0.93
AS5	70	0.3	10.96	0.89

The initial stiffness ratio of the gap at different locations with different magnitudes is shown in **Figure 16**. The initial stiffness ratio for one-side gapped models (RC5, RC10, and RC 15) and both-side gapped models (RC2.5-LC2.5, and RC5-LC5) are the same. But for model AS5, the initial stiffness ratio is lower than the model RC5 and RC5-LC5. It occurs because of the friction at the interface between the infill and the top beam. As there is no gap between the masonry infill and the top beam for models RC5 and RC5-LC5, so the top beam is expected to give extra rigidity.

The top-gapped models are already in contact with the columns, but the masonry infill is initially not in contact with the column for the side-gapped models. So, the models with top gaps (TB5, TB10, and TB15) seem to have a higher initial stiffness ratio than models with side gaps (RC5, RC10, and RC15). An 8% difference is observed in the % reduction of initial stiffness between column-gapped models (RC5, RC10, and RC 15) and the top-gapped models (TB5, TB10, and TB15).

The ultimate strength ratio of the gap at different locations with different magnitudes is shown in **Figure 17**. The ultimate strength ratio for models RC5, RC5-LC5, TB5, and AS5 is almost similar, even though their initial stiffness was different. With the increase in the size of the gap, the ultimate strength ratio reduces.

Finally, after the investigation of the gap at different locations with different magnitudes, it can be concluded that the initial stiffness is mainly affected by the gap's position at any location, while the ultimate strength is minimally impacted.

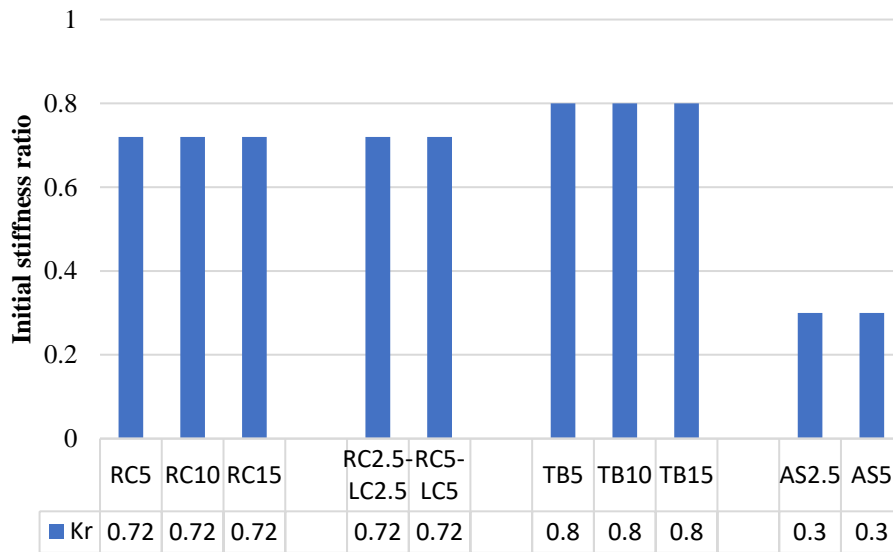


Fig. 16. Initial stiffness ratio of the gap at different locations with different magnitudes

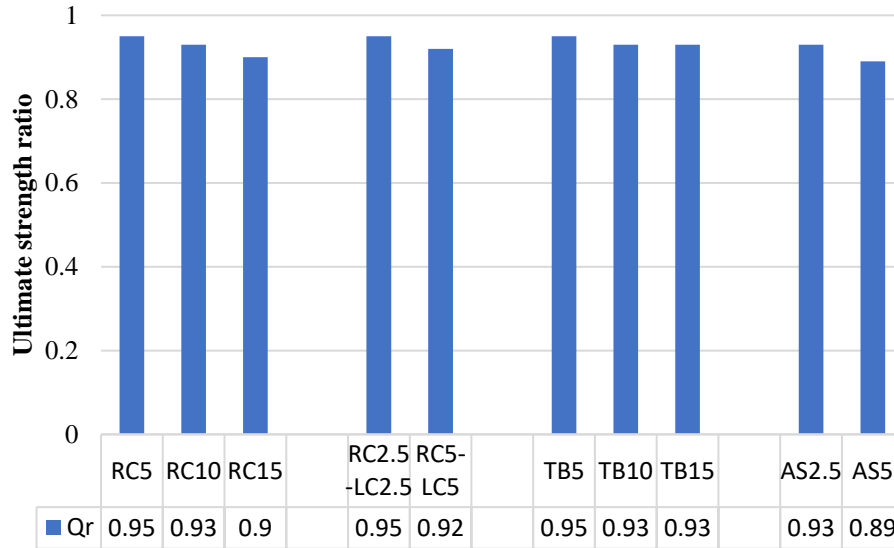


Fig. 17. Ultimate strength ratio of the gap at different locations with different magnitudes

5.6 Validation

Since there is a paucity of experimental data regarding the gap of masonry with RC frame, only one available experimental result by Hu (2015) has been utilized to validate the trend of initial stiffness and ultimate strength reduction due to gaps between masonry and RC frame. **Figure 18(a)-(b)**, shows the variation in the initial stiffness ratio ($\frac{K_{Gap}}{K_{MIF}}$) and ultimate strength ratio ($\frac{Q_{Gap}}{Q_{MIF}}$) with both sides (i.e., with both columns) gap size. It is evident that both experimental results (Hu, 2015) and FE results of this study show almost similar trends of stiffness and ultimate strength reduction.

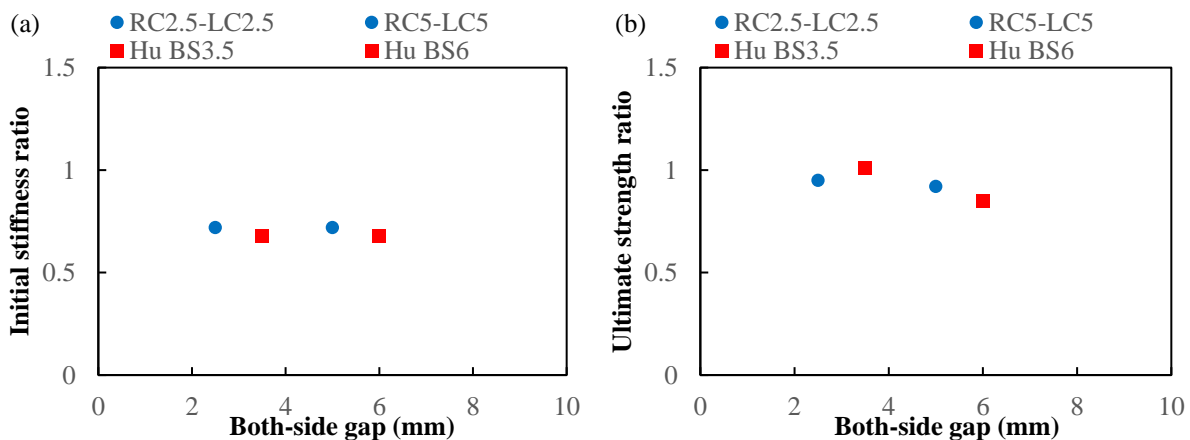


Fig. 18. Relationship between the both-side gap size and (a) initial stiffness, (b) ultimate strength for FEM and experiment (Hu, 2015)

Figure 19(a)-(b) illustrates the changes in the initial stiffness ratio and ultimate strength ratio in relation to the top gap size. The depicted data clearly indicates that there is a striking similarity in the trends of both experimental findings (Hu, 2015) and the finite element (FE) results obtained in the current study, showcasing a consistent reduction in both stiffness and ultimate strength.

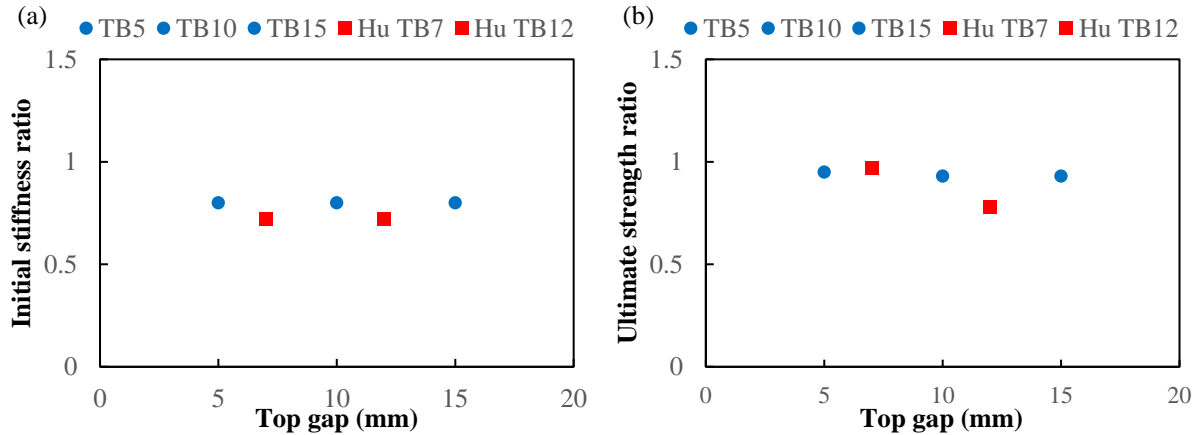


Fig. 19. Relationship between the top gap size and (a) initial stiffness, (b) ultimate strength for FEM and experiment (Hu, 2015)

6. Conclusion

In this study, a finite element analysis is performed to investigate the impact of the gap between the surrounding RC frame and the masonry infill at various locations and with varying magnitudes focused on the lateral stiffness and lateral strength of the infilled frame. Finite element modelling of one bare frame (BF) and one RC frame with masonry infill (MIF) by ABAQUS and their verification are discussed in the author's other paper (Islam et al., 2023). After the models have been validated using the experimental reference data, the identical MIF model was investigated once again with varying gap sizes at various places between the RC frame and masonry panel to study the effect of the gap. The influence of the RC frame's initial stiffness ratio and ultimate strength ratio is investigated using a parametric analysis. The following conclusions are drawn from this study:

1. In terms of initial stiffness, initially, the infilled frame with gaps at any side showed a reduction in initial stiffness when compared to an infill frame with no gaps, and this reduction was more noticeable for the gap between the infill and column (RC5, RC10, and RC15) than for the gap between infill and beam (TB5, TB10, and TB15).
2. For the gap between infill and column/columns, initial stiffness is reduced by 28%, and with the increase of the size of gaps, the ultimate strength is reduced though the reduction was less, varying from 5.09% to 9.78%.
3. The gap between the infill and beam shows a lower reduction in initial stiffness and the ultimate strength, increasing proportionally with the gap size.

4. For gaps at all interfaces, the frame initially behaves just like a bare frame. After contact, its stiffness rises and reaches its ultimate strength with a reduction varying from 6.54% to 10.96% than the masonry infill frame with no gap.
5. The position of the gap primarily influences the initial stiffness, but has little impact on the ultimate strength.
6. The obtained results distinctly suggest that there is a resemblance in the patterns observed in both the experimental results (Hu, 2015) and the finite element (FE) outcomes from the present study, demonstrating a uniform decrease in both initial stiffness and ultimate strength with the increase of top and both sides gap.

The conclusions are based on the macro model of infill masonry where the joint cracks/failure of masonry wall are not evaluated however, the trend and overall behavior of the infilled masonry frame with a gap is captured reasonably. A more detailed study would be a scope of future study.

Reference

Abaqus Documentation, (2017). Concrete damaged plasticity. Retrieved from. <https://abaqus-docs.mit.edu/2017/English/SIMACAEMATRefMap/simamat-c-concretedamaged.htm>

Abbas, R. M., and Awazli, A. G. (2017). "Behavior of Reinforced Concrete Columns Subjected to Axial Load and Cyclic Lateral Load", *Journal of Engineering*, 23(2), 21-40. <https://doi.org/10.31026/j.eng.2017.02.03>

Ali, T., Kim, R. E., Kim, K. S., and Park, K. T. (2023). "Nonlinear finite element modeling and parametric analysis for the design implication of expanded rib steel bars in RC beams", *Developments in the Built Environment*, 16, 100242. <https://doi.org/10.1016/j.dibe.2023.100242>

Alwashali, H., Suzuki, Y., and Maeda, M. (2016). "Seismic evaluation of reinforced concrete buildings with masonry infill wall", *16th World Conference on Earthquake*, Chile

Barnaure, M., and Stoica, D. N. (2015). "Analysis of masonry infilled RC frame structures under lateral loading", *Mathematical Modelling in Civil Engineering*, 11(1), 29-39. <https://doi.org/10.1515/mmce-2015-0004>

Britannica, T. Editors of Encyclopaedia (2024). İzmit earthquake of 1999. *Encyclopedia Britannica*. <https://www.britannica.com/event/Izmit-earthquake-of-1999>

BNBC (2020). *Bangladesh National Building Code*, Housing and Building Research Institute (HBRI), Bangladesh.

Carreira, D. J., and Chu, K. H. (1985). "Stress-strain relationship for plain concrete in compression", *In Journal Proceedings*, 82(6), 797-804.

Chen, X., and Liu, Y. (2017). "Finite element study of the effect of interfacial gaps on the in-plane behaviour of masonry Infills Bounded by Steel Frames", *In Structures* 10, 1-12. <https://doi.org/10.1016/j.istruc.2016.11.001>

Drucker, D.C., and Prager, W. (1952). “Soil mechanics and plastic analysis or limit design”, *Quart. Appl. Math.* 10, 157–165.

Faisal, F., Mirza, M. R., Afrin, S., and Sen, D. (2022). Modeling and Verification of Multi-Strut Modeling Approach of Masonry Panel Surrounded by RC Frame. *Journal of Engineering Science*, 13(2), 21-29. <https://doi.org/10.3329/jes.v13i2.63723>

Ferraioli, M., and Lavino, A. (2020). “Irregularity effects of masonry infills on nonlinear seismic behaviour of RC buildings”, *Mathematical Problems in Engineering*, 2020(6), 1-18. <https://doi.org/10.1155/2020/4086320>

Hu, C. (2015), “Experimental study of the effect of interfacial gaps on the in-plane behaviour of masonry infilled RC frames”, M.Sc. Thesis, University of Dalhousie, Halifax, Canada.

Islam, M. M. (2022). “A numerical study on the effect of gap between masonry infill and reinforced concrete frame under inplane loading”, M.Sc. Thesis, Ahsanullah University of Science and Technology, Bangladesh.

Islam, M. M., and Chowdhury, S. R. (2020). “Effect of gaps between infill wall and reinforced concrete frame under in plane loading – a review” *Journal of Civil and Construction Engineering*, 6(3), 1-8.

Islam, M. M., Sen, D., and Chowdhury, S. R. (2023). “Numerical investigation on the effect of infill masonry on lateral behaviour of surrounding RC frame”, *Asian Journal of Civil Engineering*, 24(8), 2851-2862. <https://doi.org/10.1007/s42107-023-00679-1>

Islam, M. T., Noor-E-Khuda, S., and Saito, T. (2022). “A simple infill frame with macro element masonry model for the in-plane performance of infill walls” *In Structures*, 42,386-404. Elsevier. <https://doi.org/10.1016/j.istruc.2022.06.014>

Kahrizi, E., Aghayari, R., Bahrami, M., and Toopchinezhad, H. (2022). On compressive stress-strain behavior of standard half-scale concrete masonry prisms. *Civil Engineering Infrastructures Journal*, 55(2), 293-307. <https://doi.org/10.22059/CEIJ.2022.324782.1758>

Kaushik, H. B., Rai, D. C., and Jain, S. K. (2007). “Stress-Strain Characteristics of Clay Brick Masonry under Uniaxial Compression.” *Journal of Materials in Civil Engineering*, 19(9), 728-739. [https://doi.org/10.1061/\(ASCE\)0899-1561\(2007\)19:9\(728\)](https://doi.org/10.1061/(ASCE)0899-1561(2007)19:9(728))

Khuda, N. E. (2022). “Reinforced masonry building under lateral loading: A numerical study”, *ACI Structural Journal*, 119(6), 83-98. <https://dx.doi.org/10.14359/51734794>

Meroni, F., Squarcina, T., Pessina, V., Locati, M., Modica, M., and Zoboli, R. (2017). “A damage scenario for the 2012 Northern Italy Earthquakes and estimation of the economic losses to residential buildings”, *International Journal of Disaster Risk Science*, 8, 326-341. <https://doi.org/10.1007/s13753-017-0142-9>

Nazief, M. A. (2014). “Finite element characterization of the behaviour of masonry infill shear walls with and without openings”, Ph.D. Thesis, University of Alberta, Canada.

Rafferty, J. P. and Pletcher, K. (2023). Sichuan earthquake of 2008. *Encyclopedia Britannica*. <https://www.britannica.com/event/Sichuan-earthquake-of-2008>

Ray, M. (2023). L'Aquila earthquake of 2009. *Encyclopedia Britannica*. <https://www.britannica.com/event/LAquila-earthquake-of-2009>, (Jun. 20, 2023).

Schäfer, B., Dörr, D., and Kärger, L. (2020). "Reduced-integrated 8-node hexahedral solid-shell element for the macroscopic forming simulation of continuous fibre-reinforced polymers", *Procedia Manufacturing*, 47, 134-139. <https://doi.org/10.1016/j.promfg.2020.04.154>

Seki, M., Popa, V., Lozinc, E., Dutu, A., and Papurcu, A. (2018). "Experimental study on retrofit technologies for RC frames with infilled brick masonry walls in developing countries", *16th European conference on Earthquake engineering*, Greece.

Sen, D., Zahura, F. T., Das, A., Alwashali, H., Islam, M. S., Maeda, M., Seki, M., and Bhuiyan, M. A. R. (2024). "A comparative investigation on experimental lateral behaviour of bare RC frame, non-strengthened and ferrocement strengthened masonry infilled RC frame". *Bulletin of the New Zealand Society for Earthquake Engineering*, 57(2), 85-96. <https://doi.org/10.5459/bnzsee.1656>

Sonpal, A. (2018). "Influence of a gap between the column and masonry wall on the response of a masonry infilled reinforced concrete frame", M.Tech. Thesis, Indian Institute of Technology, Gandhinagar, India.

Steeves, R. (2017). "In-plane behaviour of masonry infilled RC frames with interfacial gaps subjected to quasi-static loading", M.Sc. Thesis, University of Dalhousie, Halifax, Canada.

Tang, A. K., and Johansson, J. (2010). *Pisco, Peru, earthquake of August 15, 2007: lifeline performance* (pp. xvii+-214). American Society of Civil Engineers.